*35th EPS Conference on Plasma Phys. Hersonissos, 9 - 13 June 2008 ECA Vol.**32D**, P-5.049 (2008)*

Flux Core Spheromak Formation from an Unstable Screw-Pinch

Pablo L. Garcia-Martinez and Ricardo Farengo

Centro Atómico Bariloche and Instituto Balseiro, Bariloche, Argentina

Many features related to spheromak formation, sustainment, relaxation and decay have been studied in the past, using numerical simulations. Phenomena like magnetic energy relaxation, poloidal flux amplification and dynamo effect have been successfully recovered by different numerical codes (see for example Ref. [1-4]). In particular, the flux core spheromak (FCS) formation from an unstable screw-pinch has been presented by Sovinec et. al. [3]. In that work, a screw-pinch with normal magnetic field fixed at the electrodes was destabilized and sustained by the action of an axial current parallel to the flux conserver walls. In this work, we study in detail the same formation process, but introducing two differences. Firstly, we do not apply any forcing current. This feature allows us to study the relaxation event alone. Secondly, the magnetic field at the electrodes is not fixed. Instead, periodic boundary conditions are applied at the electrodes which are located at the bottom and top ends of the flux conserver, and have a smaller radius than the flux conserver.

Simulation Description

Using the VAC code, we solve the resistive isothermal MHD equations, with a shock-capturing scheme based in a Roe-type Riemann solver and a Woodward limiter [5]. The divergence-free condition of the magnetic field is maintained using the projection method [6].

In order to simplify the physics, we do not advance the density. This corresponds to a constant pressure computation, usually referred to as the zero-β (or zero-pressure) approximation, widely used when modelling low-β plasmas [3,4].

A uniform cartesian grid is used, with $N_x \times N_y \times N_z = 100 \times 100 \times 75$. The cylindrical flux conserver is constructed using appropriate values at ghost cells, i.e. knowing the solution inside the flux conserver ($r < R$), we set the values of external grid points ($r > R$) in such a way that the boundary conditions are satisfied (in $r = R$), up to the interpolation error. The perfectly conducting wall conditions employed are, $\mathbf{B} \cdot \hat{n} = 0$ and $\mathbf{J} \times \hat{n} = 0$. At the electrodes ($r < R_e$, $z = 0$ and $r < R_e$, $z = H$), periodic boundary conditions are applied.

The initial condition is a force-free screw-pinch, obtained by solving the equilibrium equation $\nabla \times \mathbf{B}(r) = \lambda(r)\mathbf{B}(r)$, with a stepwise λ profile (we used a *tanh* function in order to obtain smooth solutions) having a λ_0 value at the electrode ($r < R_e$) and zero outside ($R_e < r < R$).

The simulation presented here has cylinder radius and height of $R = 1$ and $H = 1.5$ respec-

tively, and the electrode size is $R_e = 0.35$. With this geometry, the first eigenfunction of the Taylor state is $\lambda_{Taylor} = 4.3667$. The resistivity is set to $\eta = 10^{-4}$. Following Izzo and Jarboe [4], the resistive time scale is $\tau_r = 1/\eta\lambda^2 \sim 500$. The Alfven time scale is taken to be $\tau_A = R\sqrt{\rho}/B_0 = 1$, since $\rho = 1$, and $B_0 = B_z(r = 0, t = 0) = 1$. With these parameters the Lundquist number of the simulation is $S = \tau_r/\tau_A \sim 500$.

Results and Discussion

The evolution of the total and n=0 magnetic is showed in Fig. 1a. The details of the n>0 components and kinetic energy can be observed in Fig. 1b.

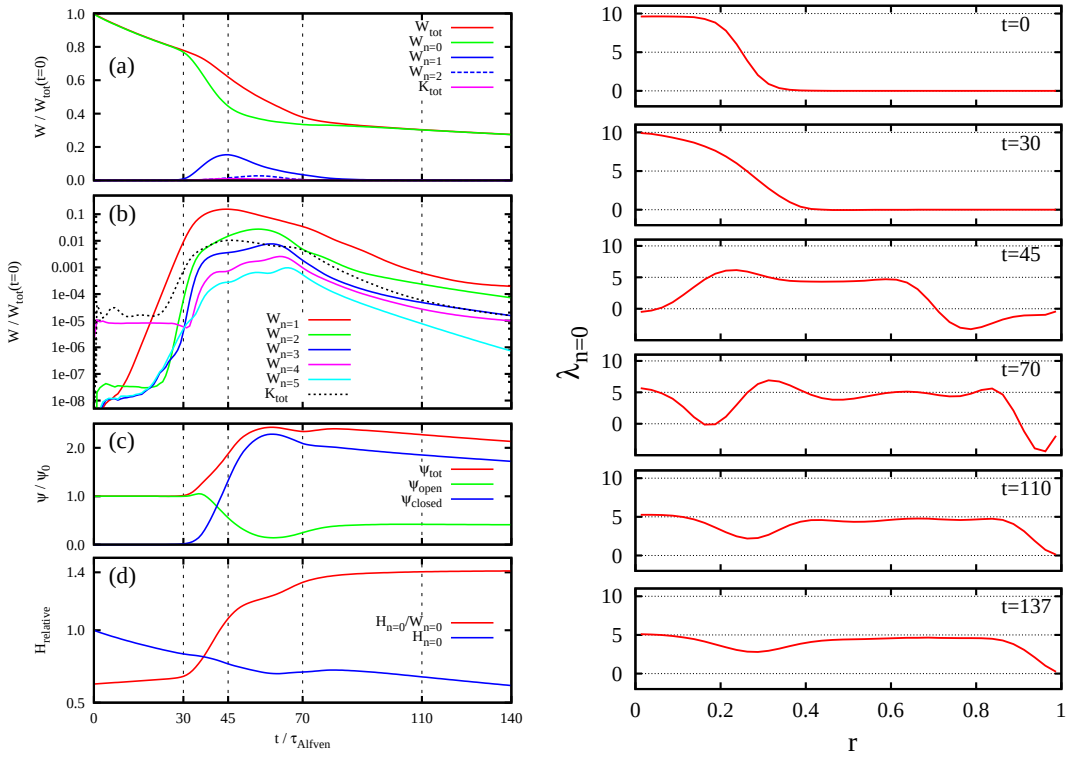

Figure 1: (Color) Evolution of magnetic energy spectrum (W_n), kinetic energy (K), poloidal flux (ψ) and relative magnetic helicity (left). Axisymmetric λ radial profiles at $z = H/2$ (right).

The complete evolution may be divided into five steps. The first step is the exponential growth of the linearly unstable n=1 mode (from $t = 0$ to $t = 30$). The second step is the nonlinear saturation of the instability, which goes from $t = 30$ to $t = 45$. A significant amount of energy is delivered from the n=0 to the n=1 mode (Fig. 1a), and also n>1 modes rapidly develop. The small amount of kinetic energy (relative to magnetic energy) involved in the relaxation process is generated during this step. The high initial value of the n=4 mode is due to the cartesian grid used. The magnetic field lines at the beginning and the end of this step are showed in Fig. 2.

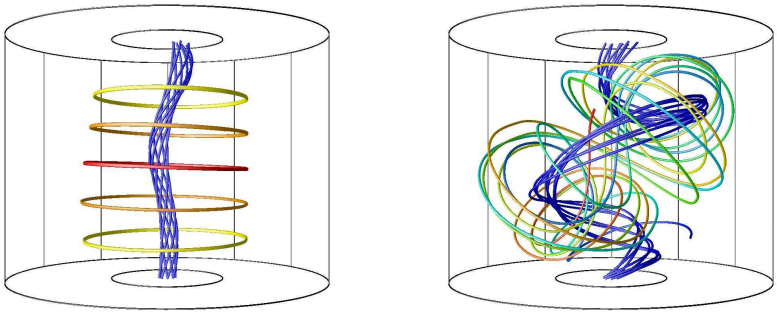

Figure 2: (Color) Magnetic field lines showing the kink instability (left) at $t = 30\tau_A$, and the non-linear saturation (right) at $t = 45\tau_A$.

In the following step (the third, from $t = 45$ to $t = 70$), the n=1 energy decreases and higher modes (n>1) are excited. This energy transfer process between modes finishes when magnetic reconnection occurs, at $t \sim 70$. The reconnection is the fourth step and it is responsible for the formation of the first closed flux tube of the spheromak (Fig. 3).

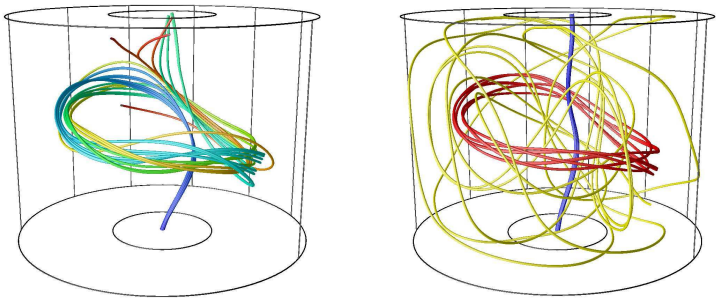

Figure 3: (Color) Field lines before the magnetic reconnection event (left) at $t = 69\tau_A$, and after reconnection (right) at $t = 71\tau_A$. The first closed flux tube is formed.

The last step involves the generation of the closed magnetic flux surfaces of the FCS configuration. After reconnection, the n>0 modes decay faster than the n=0 mode, and the configuration recovers the axisymmetry. The closed flux surfaces formation is a relatively slow process, since a small amount of n>0 activity present in the system gives rise to large stochastic regions (see field lines at $t = 110$ and $t = 137$ in Fig. 4).

In Fig.1 (right), we plot $\lambda = \mathbf{J} \cdot \mathbf{B}/B^2$ (of the n=0 mode). Initially, all the current is concentrated in the electrode zone. The MHD activity spreads the current to larger radius values and diminishes the central current ($t = 45$). Reconnection reestablishes current in the central zone ($t = 70$). In later times, the profile becomes more uniform, but a smooth variation (a minimum) remains near $r = 0.3$, where the transition from open to closed flux surfaces is located. The boundary conditions applied at the flux conserver ($\mathbf{J} \cdot \hat{t} = 0$), are responsible for the drop near $r = 1$ and the anti-parallel current observed at $t = 45$ and $t = 70$.

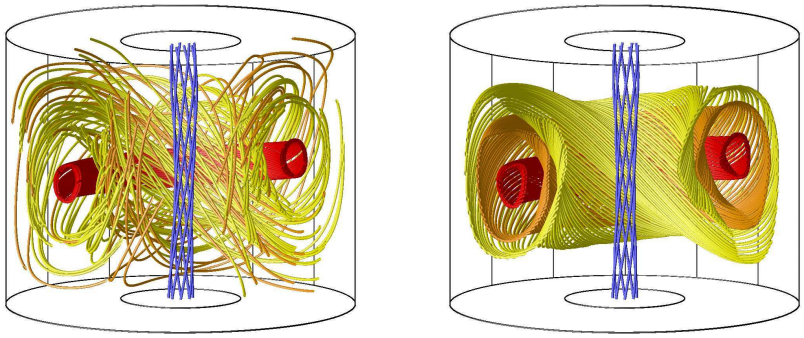

Figure 4: (Color) Formation of closed poloidal flux surfaces after reconnection, from times $t = 110\tau_A$ (left) to $t = 137\tau_A$ (right).

The safety factor (q) profile computed from this simulation is showed in Fig. 5. The q-profiles obtained in two different cases, one, varying only the flux conserver elongation from $H = 1.5$ to $H = 1.7$, and another one, varying only the electrode radius from $R_e = 0.35$ to $R_e = 0.25$, are also showed.

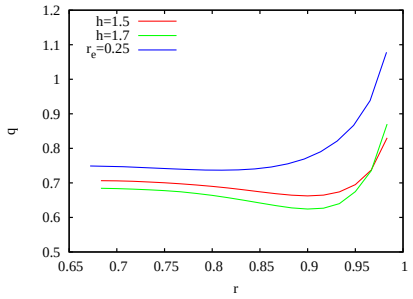

Figure 5: (Color) Safety Factor profiles for three cases.

In summary, we studied the relaxation process that produces a FCS configuration beginning from a screw-pinch, without sustainment. Five different steps were identified: linear instability, non-linear saturation, magnetic energy transfer to higher modes, magnetic reconnection and closed flux generation. The axisymmetric part of the λ profile after each step was analyzed. The resulting safety factor profile after relaxation was showed for the original case, for a case with higher elongation and for a case with smaller electrode radius.

References

[1] T. Hayashi and T. Sato, Phys. Fluids **27**, 778 (1984).

[2] K. Katayama and M. Katsurai, Phys. Fluids **29**, 1939 (1986).

[3] C. R. Sovinec, J. M. Finn, and D. del-Castillo-Negrete, Phys. Plasmas **8**, 475 (2001).

[4] V. A. Izzo and T. R. Jarboe, Phys. Plasmas **10**, 2903 (2003).

[5] VAC code, www.phys.uu.nl/∼toth/

[6] G. Tóth, J. Comput. Phys. **161**, 605 (2000).